Non-linear Dynamics of Positional Parameters of the Collimated Coherent Beam at the End of the Long Atmospheric Path

A. V. Blank[1,2], **V. V. Kapranov**[1], **R. V. Mikhailov**[2], **N. A. Suhareva**[2], **and V. Y. Tugaenko**[1]

[1]S. P. Korolev Rocket and Space Corporation "Energia", Lenin's Str. 4a, Korolev, Moscow Area, Russia
[2]Physics Faculty, Moscow State M. V. Lomonosov University, Leninskie Gory 1-2, Moscow, Russia.

Abstract— The non-linear dynamics methods were applied to the analysis of the time series of the collimated beam positional characteristics at the output of the long atmospheric path. The results are presented.The space of embedding dimension values for components of the first and second spatial moments and the structure of phase portraits, were obtained as well as Poincar recurrence time. Those allow to classify quantitatively the structure of turbulent distortions in a beam intensity distribution profile.

1. INTRODUCTION

It is difficult to describe the evolution of a complex dynamics system such as a collimated coherent beam in a nonuniform, nonstationary and nonequilibrium atmosphere using the equations of the process or to define its equations state. Even the explicit expression of the process equations allows the analytical solution of the non-linear differential equations quite rarely. Therefore the important role is played by the methods of a qualitative research of the composite systems dynamics based on experimentally recorded sequences of states. Nevertheless, for similar systems one can observe the experimental sequence of transitions in space for acceptable system state. The description of the processes observed at the output of the long atmospheric path in a phase space of variable dimension is presented. This phase space with the reconstructed trajectories gives "the portrait" of dynamic system and defines the whole set of movements arising under all possible initial and boundary conditions.

2. THE EVOLUTION OF THE COHERENT BEAM INTENSITY PROFILE

A rigorous solution of the propagation problem for a collimated coherent beam in the medium with non-stationary inhomogeneous distribution of optical density is possible on the basis of the kinetic equation for the beam Wigner function. Let us define the complex amplitude $F(\vec{r},t)$ for the given beam, here $\vec{r}$ — is the radius vector of a point in space. Wigner function for the beam complex amplitude one can put down as [1]:

$$W(\vec{r},\vec{k};t)=\left(\frac{1}{2\pi}\right)\int_{-\infty}^{\infty}F(\vec{r}+\vec{\rho},t)F^{*}(\vec{r}-\vec{\rho},t)e^{2i\vec{k}\vec{\rho}}d\vec{\rho}, \tag{1}$$

here $\vec{\rho}$ — is spatial misalignment, $\vec{k}$ — is the wave vector of the beam.

The values of the Wigner quasi-probability distribution are valid for all available space coordinates $\vec{r},\vec{k}$, but unlike traditional probability, not all the values are positive. Negative values of the distribution are typical for the states of the system inaccessible in the classical analogy. If to integrate (1) over the subspace of permissible values of spatial frequencies, one can obtain the following relations

$$\int_{-\infty}^{\infty}W(\vec{r},\vec{k},t)d\vec{k}=\left(\frac{1}{2\pi}\right)\int_{-\infty}^{\infty}\int_{-\infty}^{\infty}F(\vec{r}+\vec{\rho},t)F^{*}(\vec{r}-\vec{\rho},t)e^{2i\vec{k}\vec{\rho}}d\vec{\rho}d\vec{k}=F(\vec{r},t)F^{*}(\vec{r},t)\sim I(\vec{r},t), \tag{2}$$

which determines the probability of finding the quantum system in the vicinity the given coordinate or, in the case of wave beam — a beam intensity distribution in space. Using the Wigner distribution function allows to calculate the expected values for various physical quantities depending on the vectors coordinates and the angular frequencies. Wigner function $W(\vec{r},\vec{k})$ should also not be treated as a simultaneous probability distribution for the coordinates and momenta, because it takes a negative value. It is more justified to interpret Wigner function as an auxiliary one, satisfying many useful relations, which are often transferred to the marginal probability distributions as inheritable properties. Formula (1) actually doubles the number of independent variables, initially

used in definition of a system wave function $F(\vec{r})$. Respectively the Wigner function has the twice larger number of freedom degrees.

The sequential description of the Wigner function evolution was offered in [2]. For the case of the beam propagation in media with non-stationary and non-uniform optical characteristics, defined by the analog of potential $V(\vec{r},t)$, the equation for the Wigner function of monochromatic coherent beam takes the form:

$$\frac{\partial W(\vec{r},\vec{k},t)}{\partial t} = -\frac{k}{\omega}\frac{\partial W(\vec{r},\vec{k},t)}{\partial \vec{r}} + \frac{\partial V(\vec{r},t)}{\partial \vec{r}}\frac{\partial W(\vec{r},\vec{k},t)}{\partial \vec{k}} + \sum_{m=1}^{\infty}\frac{(i/2\pi)^{2m}}{(2m+1)!}\frac{\partial^{2m+1}V(\vec{r},t)}{\partial \vec{r}^{2m+1}}\frac{\partial^{2m+1}}{\partial \vec{k}^{2m+1}}W(\vec{r},\vec{k},t). \quad (3)$$

In the case of the relatively weak refractive distortions, allowing to maintain the approximation, analysis of the Wigner function evolution can be described by the first two terms at the right side of Equation (3). Note that the first term describes the propagation of the beam in a homogeneous isotropic medium with steady-state and homogeneous values of dielectric and magnetic conductivity. Spatial and temporal changes in the dielectric constant of the medium associated with the aerodynamic flows, under the conditions of a thermal and isobaric non-equilibrium are described by the Navier-Stokes equations for the corresponding lows of velocities and gas density changes. The analytical solution of the evolution equation for the Wigner function and, according to (2), the beam intensity distribution in the direction perpendicular to that of the cross section can be obtained only for laminar modes of aerodynamic flows. For the development of atmosphere turbulent flows any numerical analysis is generally not available because of the solutions instability of the Navier-Stokes system of nonlinear equations. The authors consider the method suggested being one of reasonable approaches to the task assigned. It allows to obtain the quantitative characteristics of stochastic processes without introducing rough simplifications and truncation. The physical model does not take into account the dissipative interactions within the system and the energy exchange with the external thermostat, respectively. And it needs to be improved for the correct description of scattering, absorption, spontaneous and induced radiation processes.

3. EMBEDDING SPACE DIMENSION

The evolution of a dynamical system one can observe in its space of states. The available modes can be obtained from its phase portrait as a set of realized in the phase space trajectories. Among them it is possible to identify a number of basic ones, determining the qualitative properties of the system. They are the points of equilibrium, corresponding to stationary mode of the system, and the closed trajectories (limit cycles), corresponding to quasi-periodic modes. The stability of a particular mode is manifested by the consistent behavior of neighboring trajectories (stable equilibrium or limit cycle attracts all nearby trajectories and repels the part of unstable trajectories). The phase portrait presented for different types of trajectory groups allows to describe all types of permissible movements for different initial conditions. In fact, the usage of the phase portraits for description of the dynamics of complex time-varying systems is reduced to the visualization of solutions of differential or difference equations of motion for a physical system [3].

In the strict definition for a system with N degrees of freedom (independent variables), one can project the feasible set of phase trajectories in the $2N$-dimensional phase space. Phase space orts, in general, correspond to the assumed function and its time derivatives. Due to uniqueness of differential equations solutions under the necessary set of initial conditions the phase trajectories in the space of the "right" dimension do not intersect [3]. The reconstructions of phase portraits show "forced" reduction of dimension, for example, when using the principal components method. Thus, taking as a bases the one-dimensional time sampling and analyzing it, one can get a complete picture of the system behavior.

Let us define the main positional parameters of the intensity distribution in the detection plane on the basis of spatial moments of the first and second orders, using (2) as follows:

$$\overrightarrow{RC}^{(1)}(t) = \frac{\int \vec{r}W(\vec{r},\vec{k};t)d\vec{r}d\vec{k}}{\int W(\vec{r},\vec{k};t)d\vec{r}d\vec{k}}, \quad \widehat{RRVar}^{(2)}(t) = \frac{\int(\vec{r}-\vec{M}_R^{(1)}(t))\times(\vec{r}-\vec{M}_R^{(1)}(t))^T W(\vec{r},\vec{k};t)d\vec{r}d\vec{k}}{\int W(\vec{r},\vec{k};t)d\vec{r}d\vec{k}}. \quad (4)$$

Note that the denominator of (4) corresponds to the registering radiation power matrix. The modulation depth of its value (or lack of it) can serve as a measure of spatial coherence degree of the

beam, provided that the video camera matrix is correctly calibrated. A series of experiments were carried out over the sloping 1000 meters path over an industrial area. Different modes of wind flows were formed depending on the season, time of day. In order to create a collimated beam a special beam positioning system was used for single-mode laser at 1064 nm wavelength. The dynamics of the intensity distributions at the output of the path was registered by high-speed camera allowing the resolution of the working field 256×256 pixel and 8-bit encoding of the intensity values and frequency of 1 kHz at a 100 µs exposure time. For each frame of video series a set of equidistant time series was defined for the two components of the vector of the first spatial moment and the three components for a symmetric tensor of the second spatial moment [4].

To analyze the nonlinear dynamic characteristics of positional beam parameters let us first of all define the embedding space dimension of processes observed using the method of false nearest neighbors. The recorded time series of positional parameters allow to create the sets of m — dimensional system state vectors at the intervals of delay d according to the following algorithm:

$$\vec{k}[i] = (k[i], k[i-d], \ldots, k[i-d(m-1)]) \tag{5}$$

d — is the interval of delay in sample rate, m — is the dimension of the vector, which should indicate the embedding space dimension.

Dimension selection is carried out by the method of false nearest neighbors [5, 6]. Let us consider a pair of vectors $\vec{k}_i^{(m)}$, $\vec{k}_j^{(m)}$, and assume these two vectors to be the neighbors in the space of dimension m. If they are true close neighbors, they will be close in the space R^{m+1} as well. The false neighbors will "disperse" in the space of a higher dimension. As a result, we get the criterion of selection the required dimension values by comparing values $||\vec{k}_i^{(m)} - \vec{k}_j^{(m)}||$ and $||\vec{k}_i^{(m+1)} - \vec{k}_j^{(m+1)}||$.

The typical dependences of the quota of false nearest neighbors on the embedding space dimension for the experimentally obtained time series of the first spatial moment under the weak turbulent perturbation modes are shown in Fig. 1. For this analysis we used statistical analysis package RStudio with additional libraries and tseriesChaos scatterplot3d. One can note almost threshold dependence of the quota of false nearest neighbors on embedding dimension. Nonmonotonic dependence in Fig. 1 in certain cases is related to the spatial inhomogeneity of the vertical movements at the atmospheric path. Larger values for the vertical positional beam component can be explained by the large number of influencing optical density external factors, especially solar radiation and vertical temperature gradients.

The estimation of the embedding space dimension is required for selection of the number of independent controlled parameters of the system to predict its evolution in the time. The result of the embedding dimension reconstruction may depend on the delay time in the creation of the system state vector. This effect is especially strong for not enough long time series [9]. The delay interval between the elements of the time series used in determining of the dimensions should be sufficient for the changing of the system state, but not sufficient for the loss of memory about the previous state. These changes are associated with the eigenfrequencies of the nonlinear dynamical system, multiple of sample rate, its harmonics and subharmonics.

4. THE PHASE PORTRAITS UNDER DIFFERENT TURBULENCE CONDITIONS

The basis reconstruction procedure of phase trajectories and attractors is formed by the Takens' theorem. It is formulated for the embeddings of compact and closed sets [7] . Let us define the embedding subset A in m-dimensional space Y as a transformation of X to Y, at which coincidence of the two images of the elements, belonging to A, is possible only in case of equality of these elements. According to the Takens' theorem, any smooth transformation X into Y will set the embedding A into Y space under the condition:

$$m \geqslant 2D_A + 1, \tag{6}$$

here D_A is fractal dimension of A set [8]. For sufficiently large samples the phase trajectories reconstructed from the time series obtain the same dimension and mathematical properties as the original physical system.

To clarity the discussion one can construct the phase trajectories family based on one-dimensional equidistant in time sample by creating the two-dimensional and three-dimensional vectors with a

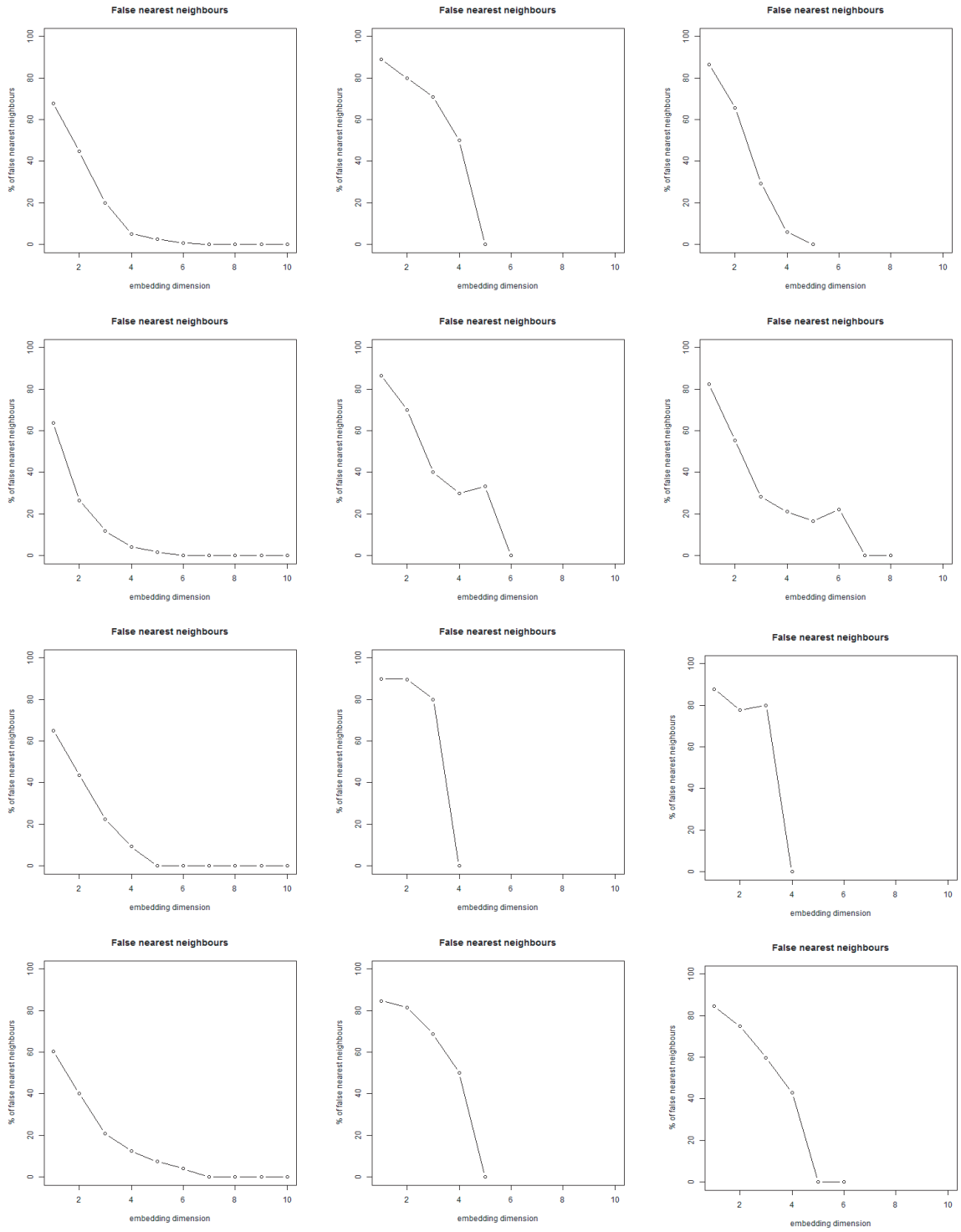

Figure 1: Dependence of the quota of false nearest neighbors from dimension of embedding space. First row — x, second row y, third row — $xxVar$, fourth row — $yyVar$.

variable time delay between the vector components [10]:

$$\begin{aligned} \vec{k}^{(2)}[i] &= (k[i], k[i-d])\,, \\ \vec{k}^{(3)}[i] &= (k[i], k[i-d], k[i-2d])\,. \end{aligned} \tag{7}$$

The phase trajectory profile depends on the ratio of the eigenfrequencies of the system analyzed

and the sampling interval. If the ratio holds true — $\tau s\omega_i = \pi/2$ (where τ — is time sampling interval, ω_i — is one of the eigenfrequencies), profile of the phase trajectory can become close to an ellipse. The optimum value of the delay interval may be selected from additional conditions, for example, according to the first minimum of the autocorrelation function of the investigated time series or a position of a mutual information local minimum [11]. For the given length of the experimental sampling N one can get $N - d(m-1)$ vectors, the set of coordinates of which forms a phase trajectory.

Examples of 3D phase portraits for turbulence modes characterized by three different values of Rytov parameter are shown in Fig. 2. Time delay d for all six reconstructions is equal to 10 ms, the coordinates of the vector components are given in millimeters.A significant difference in trajectories topology for horizontal and vertical projections is observed as well as the conspicuous eigenfrequency components for weakly developed turbulence and transformation of the beam positional characteristics to dynamic chaos mode for moderate turbulence. The same one can say about the initiation of a coherent turbulence at the highest possible values of Rytov number (for those observed in the experiment).

In a number of tasks time scans of 2D phase trajectories can be informative. They allow to

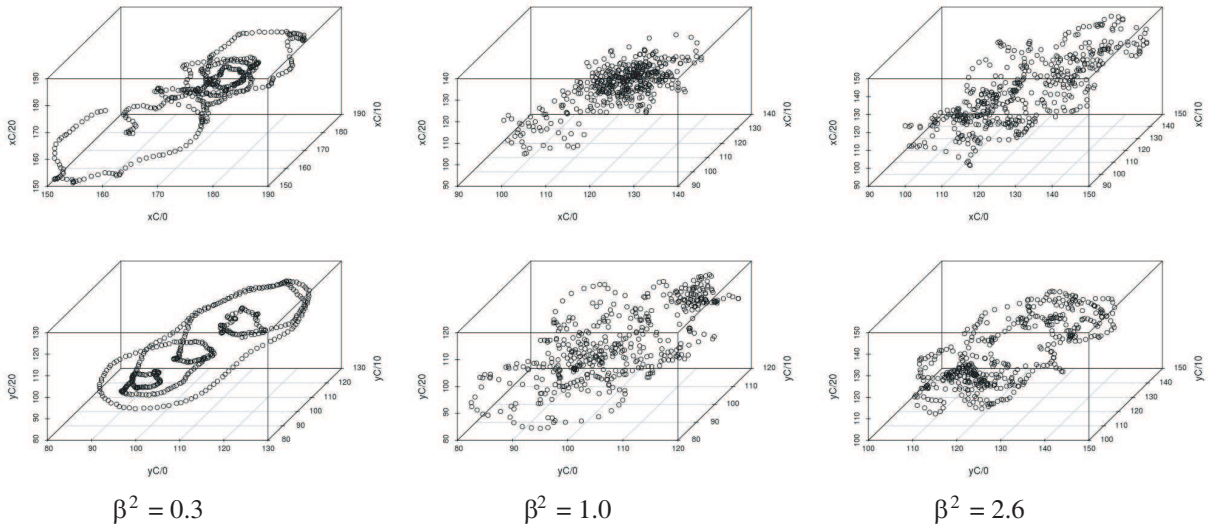

Figure 2: Phase trajectories for X (top) Y (bottom) components of the first spatial moment.

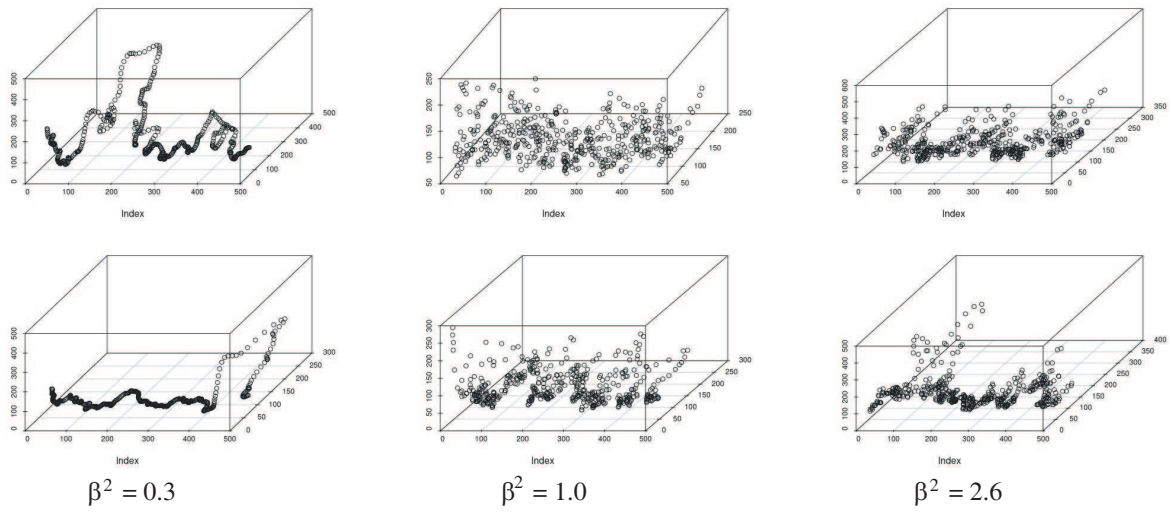

Figure 3: Time scans 2D phase trajectories XX (top) and YY (bottom) tensor components of the second central space moment of the beam.

estimate the time spent by the system in a specified phase volume and to approximate the motion near the singular points of the phase trajectories. Fig. 3 depicts a series of scans of the diagonal elements of the second central moment tensor for the intensity distribution. They manifest the single sharp refractive broadenings of the beam in different directions for low degree of the turbulence development. They are close to a Gaussian noise process of the beam size variation for medium scale of turbulence development and to the beginning of the spatial-time coordination of refractive beam distortions at the further strengthening of the turbulence over the propagation path.

5. SPECTRA OF POINCARE RECURRENCE TIMES FOR POSITIONAL PARAMETERS

The structure of the 3D and 2D + T phase trajectories for the different levels of the turbulence development over the optical path only partially reflects the dynamics of the integrated optical density modulation due to a conscientious reduction of the embedding space dimension from the values 4-5-6, as it resulted from the evaluation by the method of false nearest neighbors to the values 2-3, suitable for conventional imaging. However, to quantify the spatial-time parameters of the refractive potential $V(\vec{r}, t)$ one have to use the profiles trajectories in the space of the corresponding dimension. Properties of refractive potential are displayed in the class of available solutions, primarily in the spectrum of eigenvalues.

To restore the spectrum of eigenvalues using the reconstructed phase trajectory in the space of the appropriate dimension one applied Poincare section method. For each point of the phase trajectory it is necessary to define the Poincare recurrence time. The set of recurrence times roughly will be regarded as the range of available recurrence periods. Typical profiles of spectra for the phase trajectories of the diagonal elements of the second spatial moments in space embedding dimension $m = 5$ for different levels of the turbulence development are presented in Fig. 4.

Except the condition of poorly developed turbulence, typical for low solar activity and wind load, the spectra obtained manifest multiple distinction in the scale of the Poincare recurrence time for horizontal and vertical components of the tensor of the second spatial moments. Comparatively small number of values of recurrence times in the illustrations presented relates to restriction of number of the points processed. The extension of the recorded time series will proportionally

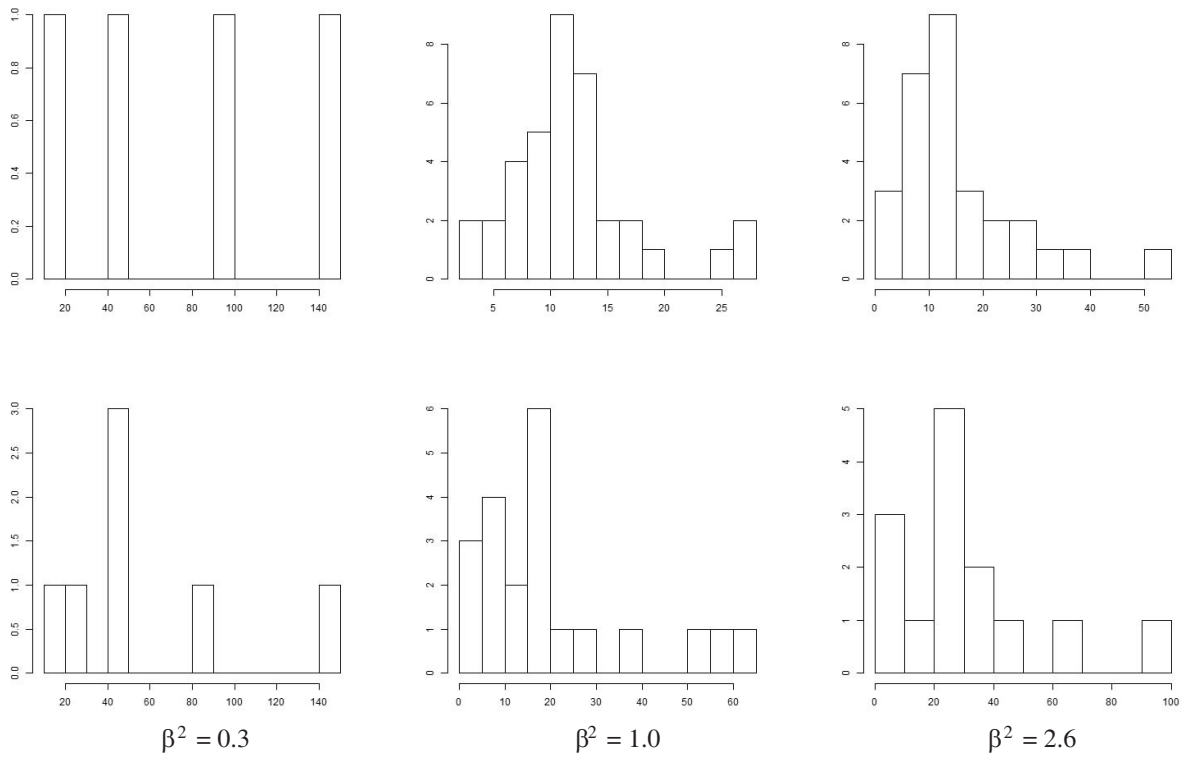

Figure 4: Spectra of Poincare recurrence times for the phase portraits of the second central spatial moments. Top — $xxVar$, bottom $yyVar$. Recurrence time is given in milliseconds.

increase "the density" of a phase portrait depiction and in a power low will increase the number of the sections satisfying the recurrence conditions .

6. CONCLUSION

The local phase portraits allow to establish the specific time scales of evolution of admissible states and eigenfrequencies of the spectrum of a stochastic process. The reconstruction and the analysis of phase portraits for stationary modes and phase trajectories for non-stationary ones becomes the basis for the method of a visual control of the dynamic modes of spatio-temporal beam aberrations as well as the classification of states of non-stationary and non-equilibrium atmosphere.

ACKNOWLEDGMENT

The work was supported by Russian Foundation for Basic Research. RFBR Project a-15-08-07484.

REFERENCES

1. Alonso, M. A., "Wigner functions in optics: Describing beams as ray bundles and pulses as particle ensembles," *Advances in Optics and Photonics*, Vol. 3, No. 4, 272–365, 2011.
2. Hillery, M. O. S. M., R. F. O'Connell, M. O. Scully, and E. P. Wigner, "Distribution functions in physics: Fundamentals," *Physics Reports*, Vol. 106, No. 3, 121–167, 1986.
3. Arnold, V. I., *Geometrical Methods in the Theory of Ordinary Differential Equations*, Vol. 250, Springer Science and Business Media, 2012.
4. Arsenyan, T. I., D. Yu. Grebennikov, N. A. Suhareva, and A. P. Sukhorukov, "Reconstruction of phase trajectories of a laser beam propagated through a turbulent medium," *Atmospheric and Oceanic Optics*, Vol. 27, No. 3, 205–210, 2014.
5. Kennel, B., R. Brown, and H. D. I. Abarbanel, "Determining embedding dimension for phase-space reconstruction using a geometrical constructions," *Phys. Rev. A*, Vol. 45, 3403, 1992.
6. Hong-Guang, M. A. and H. A. N. Chong-Zhao, "Selection of embedding dimension and delay time in phase space reconstruction," *J. Frontiers of Electrical and Electronic Engineering in China*, No. 1, 111–114, 2006.
7. Takens, F., "Detecting strange attractors in turbulence," *Lecture Notes in Math*, Vol. 898, Springer, New York, 1981.
8. Noakes, L., "The Takens embedding theorem," *International Journal of Bifurcation and Chaos*, Vol. 1, No. 4, 867–972, 1991.
9. Sauer T., J. Yorke, and V. Casdagli, "Embedology," *Journal of Statistical Physics*, Vol. 65, No. 3, 579–616, 1991.
10. Deyle, E. R. and G. Sugihara, "Generalized theorems for nonlinear state space reconstruction," *JPLoS One*, Vol. 6, No. 3, e18295, 2011.
11. Fraser A. M. and Y. L. Swinney, "Independent coordinates for strange attractors from mutual information," *Physical Review A*, Vol. 33, No. 2, 1134, 1986.